REDUCTION AND REOXIDATION OF NONTRONITE: EXTENT OF REDUCTION AND REACTION RATES

PETER KOMADEL,[1] PAUL R. LEAR,[2] AND JOSEPH W. STUCKI

Department of Agronomy, University of Illinois, Urbana, Illinois 61801

Abstract—The reduction and reoxidation of three nontronite samples, GAN (API H-33a, Garfield, Washington), SWa-1 (ferruginous Washington smectite), and NG-1 (Hohen Hagen, Federal Republic of Germany) were studied with visible absorption and Mössbauer spectroscopy. The intensity of the intervalence electron transfer (IT) band at 730 nm in these nontronites was monitored during reduction and reoxidation at 277, 294, and 348 K. The results showed that the intensity of the band followed the number of Fe(II)–O–Fe(III) groups in the clay crystal, increasing to a maximum at about Fe(II):total Fe = 0.4; upon complete reduction, the band decreased to about the intensity of the unaltered, oxidized sample. With reoxidation of the sample with O_2, the intensity of the band increased sharply, followed by a gradual decay back to the original, oxidized intensity. The ultimate level of Fe reduction achieved was at least 92%. Concomitantly, the color changed from yellow through green, blue-green, dark blue, light blue, and light gray as the Fe(II) content increased. The GAN nontronite was more difficult to reduce than the SWa-1 or NG-1 samples. The rate and level of reduction increased with the amount of reducing agent added.

Key Words—Color change, Mössbauer spectroscopy, Nontronite, Oxidation, Reduction, Visible absorption spectroscopy.

INTRODUCTION

Manipulation of the oxidation state of Fe is a potentially powerful tool in the study and utilization of clay minerals, but many applications of oxidation and reduction processes require more complete characterization of the nature and limitations of the pertinent reactions than is presently available. If octahedral Fe(III) in dioctahedral smectite is reduced to Fe(II), a number of clay properties, both physical and chemical, are altered (see review by Stucki, 1988). This phenomenon suggests that certain properties and behavior may be modified *in situ* by controlling the oxidation state. The control of Fe oxidation state in smectite would be a great benefit to many industrial, agricultural, and engineering projects, e.g., accelerating the rate of beneficiation of bentonite clays for use as drilling muds in petroleum recovery (Low *et al.,* 1983) or altering the fixation of K^+ in soils (Chen *et al.,* 1987). The oxidation state of Fe may also be used as a probe to investigate relationships between structure and physico-chemical properties of smectite, thereby improving our understanding of clay chemistry, genesis, and transformation. In spite of many years' work on Fe redox reactions in smectites, information regarding redox kinetics and reduced-state equilibria is still sketchy. The present study was conceived to address some aspects of these problems and examined the rates and extent of reduc-

tion and reoxidation of Fe in nontronites by monitoring continuously the concentration of Fe(II)-Fe(III) pairs with visible spectroscopy, supplemented by Mössbauer spectroscopy and wet-chemical methods.

MATERIALS AND METHODS

Three nontronite clays were used: NG-1 (Hohen Hagen, Federal Republic of Germany), SWa-1 (Grant County, Washington), and GAN (API H33-a, Garfield, Washington). The first two samples were obtained from the Clay Minerals Repository of The Clay Minerals Society; the last, from Ward's Natural Science Establishment, Rochester, New York. Each nontronite was fractionated to <2-μm, Na^+-saturated, washed, and freeze-dried. The magnetic Fe-oxide fraction was removed from sample NG-1 using the method of Lear *et al.* (1988).

The rate of Fe reduction and reoxidation was followed by continuously monitoring the optical density of clay suspension at 730 nm after adding a reducing or an oxidizing agent. This method is based on the intervalence electron transfer (IT) transition, which occurs between Fe(II) and Fe(III) in adjacent octahedral sites (Lear and Stucki, 1987). Twenty-five mg of sample was suspended in 2.5 ml of citrate-bicarbonate (CB) buffer solution and diluted with 37.5 ml of H_2O in an inert-atmosphere reaction vessel (Stucki *et al.,* 1984a). The suspension was then circulated (flow rate 0.14 or 0.05 ml/s) in a closed loop from the reaction vessel through a 1-cm flow cell mounted in the scattered-transmission accessory of a Beckman Model 5230 UV-Visible spectrophotometer, using a peristaltic pump (Cole-Parmer Model WZ1R057) fitted with flexible

[1] Current address: Institute of Inorganic Chemistry, CCR, Slovak Academy of Sciences, Bratislava, Czechoslovakia.
[2] Current address: EPL Bioanalytical Services, Decatur, Illinois 62525.
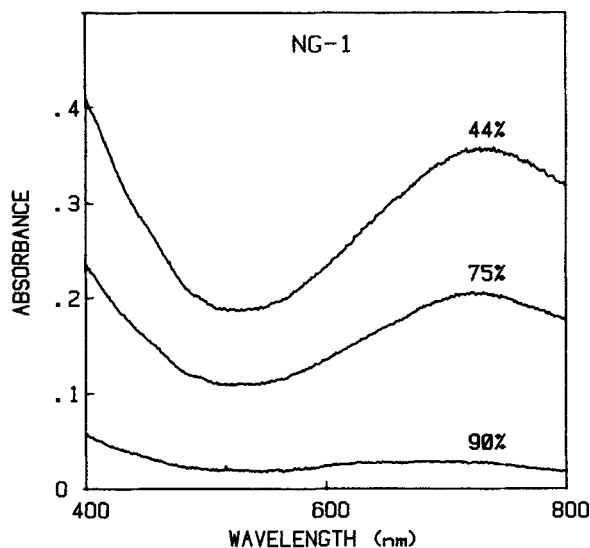
203

Figure 1. Visible absorption spectra of nontronite NG-1 in different advanced stages of reduction. Values represent percentage of total Fe reduced to Fe(II).
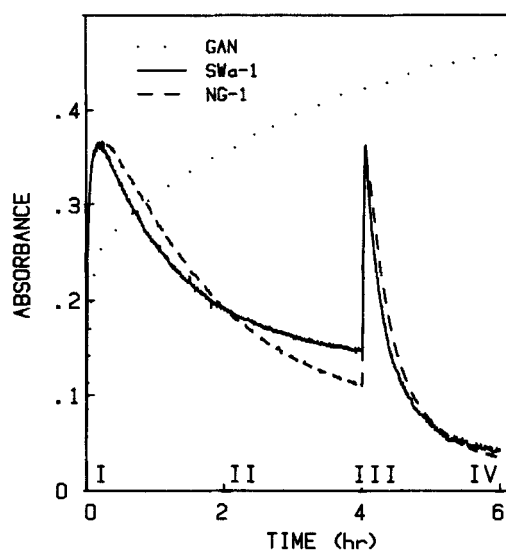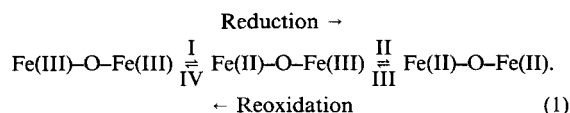

Figure 2. Rate of change of suspension absorbance at 730 nm (348 K, and flow rate of 0.14 ml/s) of nontronite samples SWa-1 and NG-1 as a result of reduction and reoxidation. Roman numerals refer to reaction stages represented in Eq. (1). The stage I reduction of sample GAN in the same time period is shown for comparison.

tubing. Six-inch, 20-gauge needles mounted to each end of the tubing provided supply and return access to the sample through the septum cap of the vessel. The atmosphere within the vessel was maintained by inserting two additional needles: one carried the purge gas (either O_2 or N_2) deep into the suspension; the other served as a vent. Purge gas was flow-regulated, then H_2O-saturated by bubbling it through a tube containing only H_2O. Gas bubbles flowing through the clay suspension furnished sufficient agitation to maintain a uniform solid:solution ratio in the optical cell. The temperature of the sample was maintained at 277, 294, or 348 K by placing the lower ⅔ of the reaction vessel in a constant-temperature water bath.

Iron was reduced by briefly removing the cap from the reaction vessel and adding solid (25, 50, or 75 mg) sodium dithionite ($Na_2S_2O_4$) directly to the clay suspension. After several hours, the purge gas was changed to O_2 to effect reoxidation. Spectral scans between 400 and 800 nm were obtained on untreated, reduced, and reoxidized samples.

Selected samples were analyzed for Fe(II) and total Fe using the 1,10-phenanthroline method of Komadel and Stucki (1988). Mössbauer spectra were obtained at 90 K using a Ranger Scientific MS-900 spectrometer equipped with a Technology Systems cryostat and analyzed with a least-squares computer program assuming Lorentzian line shapes.

RESULTS AND DISCUSSION

The visible spectrum of partially reduced nontronite in suspension is dominated by a strong intervalence transfer (IT) band centered at about 730 nm (Figure 1), which increases in intensity with the number of Fe(II)–O–Fe(III) linkages in the clay structure (Lear and Stucki, 1987). Curves showing the rate of change in intensity of this band during the reduction and reoxidation sequence of samples NG-1, SWa-1, and GAN at 348 K are presented in Figure 2. The corresponding progression of Fe–O–Fe combinations is illustrated in Eq. (1).

$$\text{Reduction} \rightarrow$$
$$\text{Fe(III)–O–Fe(III)} \underset{\text{IV}}{\overset{\text{I}}{\rightleftharpoons}} \text{Fe(II)–O–Fe(III)} \underset{\text{III}}{\overset{\text{II}}{\rightleftharpoons}} \text{Fe(II)–O–Fe(II)}.$$
$$\leftarrow \text{Reoxidation} \qquad\qquad (1)$$

Reduction

During stage I of the reduction process, the absorbance at 730 nm increased sharply immediately after addition of $Na_2S_2O_4$ and reached a maximum if the Fe(II):total Fe ratio was about 0.4 (Figure 2). The suspension changed from yellow through green to blue. All three nontronite samples behaved similarly during this initial stage, except that sample GAN failed to reach an absorbance maximum in a time period comparable to the other two samples.

The shape of the curve during stage II (Eq. (1)) varied depending on the clay, the amount of $Na_2S_2O_4$ added, and the flow rate. The maximum reducing conditions used in these experiments, i.e., 75 mg $Na_2S_2O_4$ and 348 K, produced a different level of Fe(II) in each clay in the order GAN ≪ SWa-1 < NG-1 (Figure 2). The
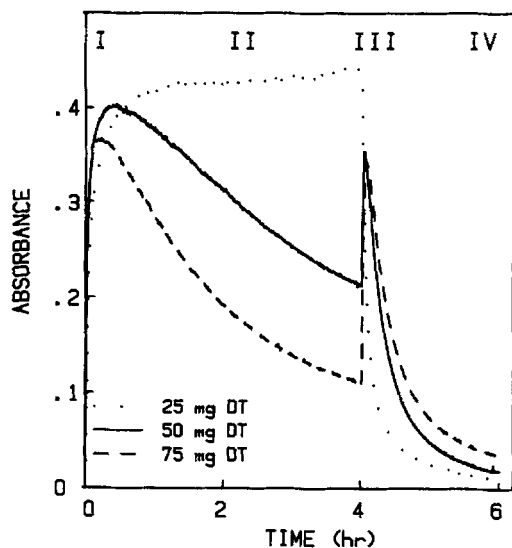
Figure 3. Effect of amount of reducing agent ($DT = Na_2S_2O_4$) on the rate and extent of reduction and reoxidation of nontronite NG-1 at 348 K, 0.14 ml/s. Absorbance was measured at 730 nm. Roman numerals refer to reaction stages represented in Eq. (1).
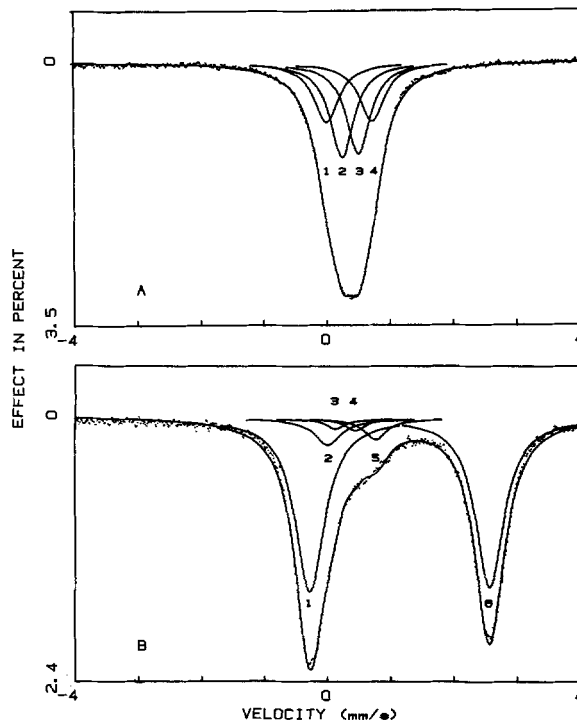

Figure 4. Mössbauer spectra of unaltered (A) and reduced (B) nontronite NG-1 at 90 K. Peaks 1 and 6 in (B) are assigned to Fe(II); all others in (A) and (B) are assigned to Fe(III). Spectral parameters are reported in Table 1.

curves for samples NG-1 and SWa-1 were similar, but the addition of 75 mg $Na_2S_2O_4$ to sample GAN was insufficient to produce an absorbance maximum within 7 hr (giving a $t_{1/2}$ of >11,400 s at 348 K), which demonstrates that sample GAN was more difficult to reduce than the other two samples. This result compares favorably with the findings of Stucki et al. (1984a) that 75 mg of $Na_2S_2O_4$ reduced less than one-third of the Fe in sample GAN in an unpurged reaction vessel, and that even 200 mg of this material failed to reduce more than half of the Fe. Russell et al. (1979) observed that a 10-min treatment of different nontronite films with $Na_2S_2O_4$ solution produced the least reduction in sample GAN.

The cause of the unique behavior of sample GAN compared to samples NG-1 and SWa-1 is unknown, but likely was due to subtle variability in layer composition, expansion properties, and ordering of structural cations, all of which would have influenced the accessibility of the reducing agent to octahedral Fe. Little is known about the differences in these variables among nontronite samples, so one can do little more than speculate. The swelling pressure of sample GAN (Stucki et al., 1984b), however, dropped much more sharply with increasing Fe(II) content than did that of sample SWa-1 (Lear and Stucki, 1987), indicating that the layers in sample GAN collapsed (Lear and Stucki, 1989) more readily, which, assuming a diffusion-controlled mechanism, would have retarded the rate and even the extent of reduction.

Another possible factor is a difference in tetrahedral

Fe content. Russell et al. (1979) found a direct correlation between the amount of Fe reduced after a fixed-time exposure to reducing agent and the tetrahedral Fe content of a nontronite series, suggesting that the transition metal in tetrahedral sheets facilitates electron transfer. But the tetrahedral Fe content of samples GAN and SWa-1 (Goodman et al., 1976; Bonnin et al., 1985) appears to be too similar for this to be an important variable in the present study. Finally, the total Fe contents of samples SWa-1 and GAN are 3.595 and 4.201 mmole/g, respectively, suggesting less possibility for disorder in the distribution of structural cations in sample GAN than in sample SWa-1; however, the role this difference may have played in reduction is unclear.

The addition of increasingly greater amounts of $Na_2S_2O_4$ clearly increased the reducing ability of the system, which ultimately produced very high levels of Fe(II) and a very low suspension absorbance in samples NG-1 and SWa-1, as illustrated in Figure 3 (stage II). In the more highly reduced suspensions, the color continued to change with time, progressively from dark blue to light blue then light gray.

Chemical analysis and Mössbauer spectra of oxidized and reduced samples of nontronite NG-1 (Figure 4 and Table 1) confirm that this spectral progression through stages I and II was the result of increasing

Table 1. Calculated parameters from Mössbauer spectra (Figure 4) of oxidized (unaltered) and reduced nontronite NG-1 at 90 K.

Treatment	Peaks	IS (mm/s)	QS (mm/s)	Γ (mm/s)	Area/ total area (%)	Oxidation state of Fe
Unaltered	1, 4	0.32	0.72	0.48	42	Fe(III)
	2, 3	0.33	0.25	0.44	58	Fe(III)
Reduced	1, 6	1.07	2.85	0.57	85	Fe(II)
	2, 5	0.36	0.84	0.43	10	Fe(III)
	3, 4	0.15	0.49	0.50	5	Fe(III)

IS = isomer shift; QS = quadrupole splitting; Γ = full-width at half maximum.

Fe(II) content, which first increased then decreased the number of Fe(II)–O–Fe(III) combinations in the structure. The light-gray product obtained after 4 hr of reduction was probably almost all Fe(II). Chemical analysis of this sample showed 92% of the total Fe to be Fe(II), even after freeze-drying (a process that likely invoked some reoxidation). The Mössbauer spectrum showed at least 85% Fe(II) (Figure 4B). Such high levels of Fe reduction were possible because of the higher temperature (348 K) and the continuous flow of N_2 through the suspension, which swept gaseous reaction products out of the system and thereby permitted the reaction to continue to completion.

The greater reduction potential attained by increasing the concentration of reducing agent was also reflected in the curves as a slight decrease in the absorbance maximum (Figure 3). Indeed, the intensity of the absorbance maximum varied inversely with the amount of $Na_2S_2O_4$ added. Note also that the time needed to achieve these maxima also decreased with increasing $Na_2S_2O_4$, probably because at higher reduction rates or potentials some Fe(II)–O–Fe(II) pairs were established before all Fe(III)–O–Fe(III) groups were partially reduced to Fe(II)–O–Fe(III). In other words, the reduction reactions illustrated in Eq. (1) probably did not occur in an orderly sequence in which each step was completed before the next step began. The intermediate, mixed-valent species may either have been short-lived or was never present in some regions of the crystal. Such a non-sequential progression of reactions could occur, for example, if a uniform distribution of Fe(II)–O–Fe(III) pairs were dependent, at least in part, on a redistribution of Fe(II) and Fe(III) in the structure by means of electron mobility or hopping from one Fe center to the next. If such a process occurred and were slower than the initial electron transfer into the crystal, increasing the rate of initial electron transfer, e.g., by raising the concentration of reducing agent, would have forced the reaction (Eq. (1)) beyond the intermediate step. On the opposite end of the rate scale, using 25 mg $Na_2S_2O_4$, the very slow absorption increase and the failure to reach an ab-
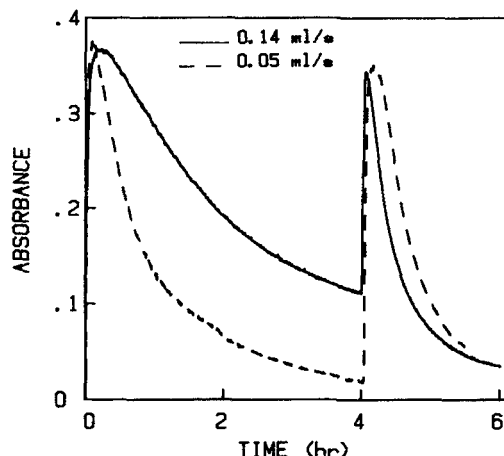

Figure 5. Effect of flow rate on the rate and extent of reduction and reoxidation of nontronite NG-1 with 75 mg $Na_2S_2O_4$ at 348 K. Absorbance was measured at 730 nm.

sorption maximum in 1 to 4 hr (Figure 3) could have been caused by competitive reoxidation within the sample due to leakage around needle and tube joints.

The visible absorption spectra of partly and highly reduced samples (Figure 1) also illustrate that, in addition to the loss of intensity of the IT bands, the absorbance level of the entire spectrum decreased on reduction of the sample. This result was likely due to the loss of other Fe(III) peaks, such as the O → Fe(III) charge-transfer band centered at 260 nm which tails into the visible range (Karickhoff and Bailey, 1973), or to Fe(III) clusters (Sherman and Vergo, 1988). Reduction would have diminished either of these types of resonance, resulting in lower absorbance background.

The influence of flow rate on the shape of the absorbance-time curves of sample NG-1 is shown in Figure 5. Using the same amount of reducing agent (75 mg $Na_2S_2O_4$), reduction was faster and more complete with the slower flow rate of 0.05 ml/s, but slight sedimentation in the spectrophotometer flow cell precluded the use of this rate for samples SWa-1 or GAN. Either flow rate (0.05 or 0.14 ml/s) could be used for sample NG-1. The apparatus used to circulate sample suspensions was incapable of providing complete insulation of the reaction mixture from atmospheric O_2 because of rather large differences between the tubing and needle diameters. This lack of complete insulation was particularly noticeable at the higher flow rate, with which some bubbles were visible in the lines and undoubtedly caused some reoxidation of Fe(II) and/or oxidation of the reducing agent.

Reoxidation

The substitution of O_2 for N_2 in the purge-gas stream after 4 hr of reduction brought about immediate, rapid reoxidation during stage III (Figures 2 and 3), causing

the absorbance to increase rapidly to a maximum with the initial conversion of Fe(II)–O–Fe(II) to Fe(II)–O–Fe(III). The rate of reoxidation in this stage was sharper than the rate of reduction in stage II. Reoxidation continued steadily through stage IV until only Fe(III)–O–Fe(III) remained, and the original yellow color of the suspension was restored. No red or orange color, such as observed by Rozenson and Heller-Kallai (1976) and Stucki (unpublished) in reoxidized products of samples reduced without pH buffering, was present. Reoxidation of sample GAN (not shown) followed a similar pattern to that of samples SWa-1 and NG-1, except, because reduction failed to exceed 50% in sample GAN, the initial absorbance spike at stage III was absent.

Formal kinetics

The absolute value of absorbance was used as the measure of the concentration of Fe(II)–O–Fe(III) combinations at lower temperatures. At 277 or 294 K no maximum appeared on the absorbance *vs.* time curves during either the course of reduction or in the course of reoxidation, even if 75 mg $Na_2S_2O_4$ was used. The curves were similar to the curve for 25 mg $Na_2S_2O_4$ at 348 K for sample NG-1 (Figure 3).

Attempts were made to fit the experimental rate data to standard laws of reaction kinetics, but failed to yield a rational reaction order. This result is understandable considering the many factors entering into the process that could neither be controlled precisely nor characterized completely, e.g., the time delay ($\sim$30 s) in transferring the suspension from the reactions vessel to the spectrophotometer.

The half-times ($t_{1/2}$) of reduction and reoxidation, as given by the quantity of Fe(II)–O–Fe(III) combinations in the crystal, were calculated as a measure of reaction rate according to the relation

$$t_{1/2} = (A_1 - A_2)/2, \qquad (2)$$

where A_1 is the maximum absorbance observed in the analysis for both reduction and reoxidation, A_2 is the absorbance at $t = 0$ for reduction or the absorbance after 1-hr purge with O_2 for reoxidation (Figures 1 and 2).

Reduction reaction rates for nontronite samples NG-1 and SWa-1 increased with temperature (Table 2). Sample SWa-1 was reduced faster than sample NG-1 at both 277 and 294 K. Reoxidation was very fast at both temperatures. For a more exact kinetic study of these reactions, a modified apparatus will be needed.

CONCLUSIONS

The color of Fe-rich smectite clearly is indicative of the level of Fe(II) in the crystal structure because of the intervalence electron transfer (IT) bands which occur due to mixed and variable oxidation states of Fe in octahedral sites. The most frequently observed color is green or blue-green, which occurs if Fe(II) and Fe(III)

Table 2. Half-times of reduction and reoxidation of nontronite samples NG-1 and SWa-1 at 277 and 294 K.[1]

Nontronite	Chemical process	Temperature (K)	$t_{1/2}$ (s)
NG-1	Reduction	277	1760 ± 70
		294	900 ± 70
	Reoxidation	277	<250
		294	<250
SWa-1	Reduction	277	1370 ± 40
		294	680 ± 80
	Reoxidation	277	280 ± 100
		294	<250

[1] 75 mg $Na_2S_2O_4$ and flow rate 0.14 ml/s were used.

are present in adjacent sites; complete reduction, however, produces a light-gray product. The colors indicate that electrons become more mobile or delocalized in the crystal structure during reduction, which, in turn, can alter the electron density distribution in the crystal and increase the polarizability of electrons in orbitals of surface oxygen ions. Shifts in electron density and polarizability are important in understanding how Fe(II) governs and controls surface properties of the clay because these properties influence hydrogen bonding, van der Waals, and surface hydration forces.

The fact that these three, similar nontronites (GAN, SWa-1, and NG-1) behaved differently in their reduction reactions is an exciting prospect for future research. Although the differences in the observed rates and levels of reduction have yet to be explained, as these clays become more fully characterized in suspension, the site at which the reducing agent approaches the clay layer may be identified and the mechanism of electron transfer into the octahedral sheet may be revealed. As better methods for following the reaction kinetics are developed, the kinetic parameters of the reduction reaction may also be found, which will greatly clarify the precise reactions involved in the reduction process.

ACKNOWLEDGMENTS

REFERENCES

Bonnin, D., Calas, G., Suquet, H., and Pezerat, H. (1985) Site occupancy of Fe^{3+} in Garfield nontronite: A spectroscopic study: *Phys. Chem. Minerals* **12**, 55–64.

Chen, S. A., Low, P. F., and Roth, C. B. (1987) Relation between potassium fixation and the oxidation state of octahedral iron: *Soil Sci. Soc. Amer. J.* **51**, 82–86.

Goodman, B. A., Russell, J. D., Fraser, A. R., and Woodhams, F. W. D. (1976) A Mössbauer and I.R. spectroscopic study of the structure of nontronite: *Clays & Clay Minerals* **24**, 53–59.

Karickhoff, S. W. and Bailey, G. W. (1973) Optical absorp-

tion spectra of clay minerals: *Clays & Clay Minerals* **21,** 59–70.

Komadel, P. and Stucki, J. W. (1988) The quantitative assay of minerals for Fe^{2+} and Fe^{3+} using 1,10-phenanthroline. III. A rapid photochemical method: *Clays & Clay Minerals* **36,** 379–381.

Lear, P. R., Komadel, P., and Stucki, J. W. (1988) Mössbauer spectroscopic identification of iron oxides in nontronite from Hohen Hagen, Federal Republic of Germany: *Clays & Clay Minerals* **36,** 376–378.

Lear, P. R. and Stucki, J. W. (1987) Intervalence electron transfer and magnetic exchange interactions in reduced nontronite: *Clays & Clay Minerals* **35,** 373–378.

Lear, P. R. and Stucki, J. W. (1989) Effect of iron oxidation state on the surface area of smectites: *Clays & Clay Minerals* **37,** (in press).

Low, P. F., Roth, C. B., and Stucki, J. W. (1983) System and method for rapid beneficiation of bentonite clay: *U.S. Patent* **4,411,530,** 4 pp.

Rozenson, I. and Heller-Kallai, L. (1976) Reduction and oxidation of Fe^{3+} in dioctahedral smectites—1: Reduction with hydrazine and dithionite: *Clays & Clay Minerals* **24,** 271–282.

Russell, J. D., Goodman, B. A., and Fraser, A. R. (1979) Infrared and Mössbauer studies of reduced nontronites: *Clays & Clay Minerals* **27,** 63–71.

Sherman, D. and Vergo, N. (1988) Optical (diffuse reflectance) and Mössbauer spectroscopic study of nontronite and related Fe-bearing smectites: *Amer. Mineral.* **73,** 1346–1354.

Stucki, J. W. (1988) Structural iron in smectites: in *Iron in Soils and Clay Minerals,* J. W. Stucki, B. A. Goodman, and U. Schwertmann, eds. D. Reidel, Dordrecht, The Netherlands, 625–675.

Stucki, J. W., Golden, D. C., and Roth, C. B. (1984a) The preparation and handling of dithionite-reduced smectite suspensions: *Clays & Clay Minerals* **32,** 191–197.

Stucki, J. W., Low, P. F., Roth, C. B., and Golden, D. C. (1984b) Effect of iron oxidation state on clay swelling: *Clays & Clay Minerals* **32,** 357–362.